

ABAB Homoleptic Bis(phthalocyaninato)lanthanide(III) Complexes: Original Octupolar Design Leading to Giant Quadratic Hyperpolarizability

Mehmet Menaf Ayhan,^{†,||} Anu Singh,[⊥] Erwann Jeanneau,[§] Vefa Ahsen,[†] Joseph Zyss,[⊥] Isabelle Ledoux-Rak,[⊥] Ayşe Gül Gürek,[†] Catherine Hirel,^{*,†} Yann Bretonnière,^{*,||} and Chantal Andraud^{||}

[†]Department of Chemistry, Gebze Institute of Technology, P.O. Box 141, 41400 Gebze, Kocaeli, Turkey

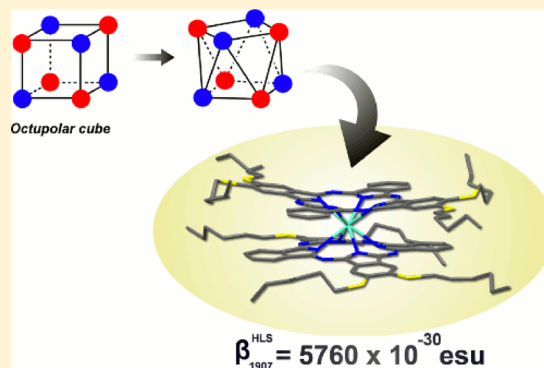
[§]Centre de Diffractométrie Henri Longchambon, Université Lyon I, 43 boulevard du 11 Novembre 1918, 69622 Villeurbanne Cedex, France

[⊥]ENS-Cachan, Institut D'Alembert, CNRS UMR 8537, ENS Cachan, 61 avenue du Président Wilson, 94235 Cachan Cedex, France

^{||}Laboratoire de Chimie de l'ENS de Lyon, CNRS UMR 5182, Université Lyon I, ENS de Lyon, 46 allée d'Italie, 69364 Lyon cedex 07, France

Supporting Information

ABSTRACT: The octupolar cube, a T_d symmetry cube presenting alternating charges at its corners, is the generic point charge template of any octupolar molecule. So far, transposition into real molecular structures has yet to be achieved. We report here a first step toward the elaboration of fully cubic octupolar architectures. A series of octupolar bis(2,3,16,17-tetra(hexylthio)phthalocyaninato)lanthanide double-decker complexes $[\text{Pc}_2\text{Ln}]$, Ln = Nd (1), Eu (2), Dy (3), Y (4), and Lu (5), are described, whose original three-dimensional structures display the required alternation of ABAB type for one face of the cube and the delocalization between the two rings approximating to the electronic interaction along the edges of the cube. Synthesis, X-ray crystal structure, and study of the optical properties and of the first molecular hyperpolarizability β are reported. The size of the lanthanide (III) central ion modulates the ring-to-ring distance and the degree of coupling between the two phthalocyanine rings. As a consequence, the optical properties of these octupolar chromophores and in particular the strong near-infrared absorption due to the intervalence transition between the two rings also depend on the central lanthanide (III) ion. The first oxidized and reduced states of the complexes, while keeping a similar octupolar structure, display considerably changed optical properties compared to the neutral states. Second-order nonlinear properties were determined by nonpolarized harmonic light scattering in solution at 1907 nm. Exceptionally large dynamic molecular first hyperpolarizabilities $\sqrt{\langle \beta_{\text{HLS}}^2 \rangle_{1907}}$, among the highest ever reported, were found that showed a strong dependence on the number of 4f electrons.



INTRODUCTION

The design of second-order nonlinear optical molecules mainly focused on one-dimensional (1D) dipolar push–pull molecules with a charge transfer polarized along the molecular axis z . Extensive molecular engineering around this [donor]–[electronic conjugated pathway]–[acceptor] structure combining the increase of the donor or acceptor strength, the modification of the electronic structure of the conjugated path, or the adequate combinations of the end donor and acceptor groups with the conjugated bridge led to very large molecular factors of merit $\mu\beta$.¹ This restricted template, however, where only the on-axis component β_{zzz} is nonzero, failed to take into account the three-dimensional (3D) nature of the hyperpolarizability tensor β . Studies based on group theory and quantum mechanics have helped set conceptual foundations to the domain of nondipolar molecules for nonlinear optics, which

became known as *octupolar* and more generally *multipolar* molecules.² Octupolar molecules in which symmetry constraints impose a cancellation of the dipole moment have considerably extended the possibilities of molecular design by enlarging the dimensionality of the charge transfer. At a structural level it was shown that the most generic template for octupolar molecules was a cube of symmetry T_d presenting alternating charges at the corners (Figure 1).^{2,3} More specific arrangements eventually with reduced dimensionality can be deduced from this basic cubic point charge template by projecting the charges on the center of the cube along the C_3 diagonal axis or by fusion of one type of charge in the barycenter of the cube. The transposition of these point charge

Received: December 24, 2013

Published: March 5, 2014

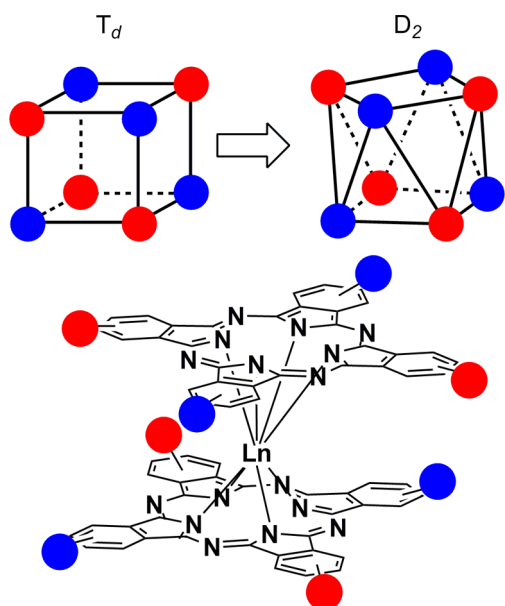


Figure 1. Bis(phthalocyanines)lanthanide complexes $[\text{Ln}^{\text{III}}(\text{Pc})(\text{Pc}^*)]$ as point-charge template for octupole.

templates into real structures has given rise to a realm of original octupolar molecules⁴ that includes purely organic D_{3h} tri- or hexa-substituted aryl compounds,⁵ propeller-like D_3 molecules built on a functionalized trivalent carbon^{5c,6} or nitrogen atom,⁷ tetrahedral (T_d) tetra-substituted carbon, silicon, and phosphorus derivatives,⁸ D_{2d} functionalized biphenyl derivatives,⁹ or boron subphthalocyanines (C_{3v}),¹⁰ to cite a few. Coordination chemistry further extended the possibilities of engineering nondipolar architectures. Following the early work of Zyss on D_3 $[\text{Ru}(\text{bpy})_3]^{2+}$,¹¹ a large number of metal complexes and organometallic octupolar structures have been described. Good examples of these are covalent tetrahedral (T_d) tin derivatives,¹² D_{2d} or D_3 metal complexes of bipyridyl ligands¹³ or lanthanide tris(bipyridine) or dipicolinate complexes,¹⁴ in which not only the template effect of the metal ion was exploiting to create noncentrosymmetric structures, but the intrinsic properties of the metal ion and of the metal-to-ligand specific transition were taken advantage of to tune the electronic and optical properties of the final object. Very recently, Ru(II)terpyridyl complexes combined with zinc(II) porphyrinato units were used to create octupolar molecules having impressive β_{HRS} ($>1000 \cdot 10^{-30}$ esu) values at telecommunication-relevant wavelength (1300 nm).¹⁵ However, despite the huge number of octupolar structures reported the translation of the ideal figure into a real “cubic” molecule (even if deformed) with eight alternated charges at the corner and delocalization of the charges between the higher and lower planes has yet to be realized. Taking advantage of the unconventional through-space intramolecular charge transfer provided by the paracyclophane framework, Bazan et al.¹⁶ described the closest example thus far. However, the cubic scheme was not complete as only half a cube has been obtained with substitution consisting of four donor (respectively acceptor) groups on the paracyclophane moiety only.

With various ions and especially with lanthanide(III) ions,¹⁷ phthalocyanines form sandwich-type complexes in which the metal ion holds two macrocycles closer than their van der Waals distance, resulting in strong π - π interactions and through-space 3D delocalization. The nature of these

compounds has been the subject of long debate. Electron spin resonance and theoretical calculations on lutetium(III) bis(phthalocyaninate) correlated to absorption spectroscopy experiments¹⁸ demonstrated the existence of an unpaired electron completely delocalized over both rings. The now commonly accepted structure of lanthanide bis-(phthalocyaninates) is a neutral radical in which one macrocycle is twice negatively charged, whereas the other is a doubly deprotonated π radical $[\text{Ln}(\text{Pc})(\text{Pc}^*)]$ where the term Pc stands for doubly deprotonated phthalocyanine ring. The unpaired electron is delocalized over the two cycles on the semi-occupied SOMO.^{18b,19}

X-ray diffraction studies on $[\text{Nd}^{\text{III}}(\text{Pc})(\text{Pc}^*)]$ and $[\text{Lu}^{\text{III}}(\text{Pc})(\text{Pc}^*)]$ ²⁰ showed that the two rings in the sandwich complex were staggered by around 45° , giving a noncentrosymmetric structure of D_{4d} symmetry. We put forward that lanthanide complexes with crosswise ABAB macrocycles featuring alternating electron donor and electron acceptor groups could give an almost exact representation of the octupolar cube (Figure 1), the delocalization between the two rings approximating to the electronic interaction along the edges of the cube. This idea was illustrated in a preliminary communication,²¹ in which we described the synthesis, the molecular structure, and the measure of the molecular first-order hyperpolarizability β of such a complex, with the example of the lutetium sandwich complex of 2,3,16,17-tetra(hexylthio)phthalocyanine, an ABAB crosswise phthalocyanine, bearing electron donor (thioalkyl) groups on two opposite rings. Although we were aware that there were no real electron accepting groups, the required alternation of ABAB type for one face of the cube was present as thioalkyl, and hydrogen atoms do not have the same electronic effect. An exceptionally high value of 5750×10^{-30} esu for the molecular first-order hyperpolarizability β was measured at 1907 nm, stressing that this molecular design could lead to very efficient and original octupolar molecules.

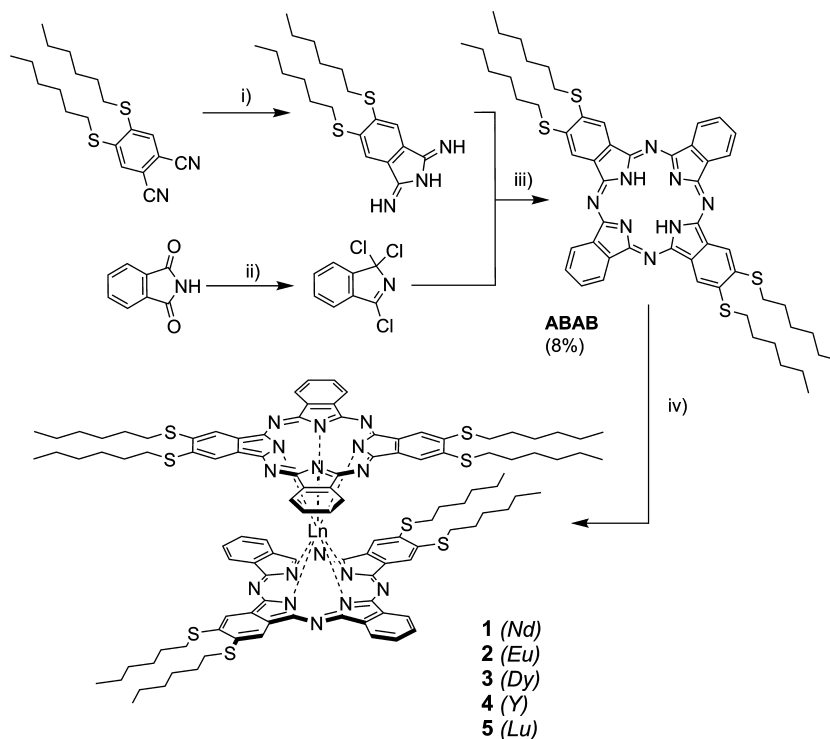
In this article, we wish to extend the chemistry to rare earth ions of representative ionic size (Nd, Eu, Dy, Y) chosen to provide a variation in the degree of coupling between the phthalocyanine rings and as a consequence in the energy of the intervalence transition, to gain a better understanding of the second-order nonlinear optical properties observed. Thus, the synthesis, the X-ray crystal structure, and the study of the optical properties and of the first molecular hyperpolarizability β of various (2,3,16,17-tetra(hexylthio)phthalocyaninato)lanthanide complexes $[\text{Ln}^{\text{III}}(\text{Pc})(\text{Pc}^*)]$, Ln = Nd (1), Eu (2), Dy (3), Y (4), and Lu (5) are reported. The first oxidized and reduced states of the complexes presenting very different optical properties than the neutral states are also investigated.

EXPERIMENTAL SECTION

General. Starting materials were purchased from Aldrich, Fluka, and Alfa and were used without further purification unless otherwise stated. Residual water in lanthanide acetate salts $\text{Ln}(\text{OAc})_3$ was removed by heating at 120°C under vacuum (10^{-2} mmHg) for one week. 2,3,16,17-tetra(hexylthio)phthalocyanine was prepared as previously described.²¹ ^1H NMR spectra were recorded on a Bruker Avance 300 spectrometer. High-resolution mass-spectrometry (HR-MS) experiments were performed at the center commun de spectrométrie de masse from Université Claude Bernard Lyon I on a MicroTof-Q Bruker mass spectrometer. Electronic absorption spectra were recorded on a Jasco V770 spectrophotometer.

(2,3,16,17-Tetra(hexylthio)phthalocyaninato)lanthanide $[\text{Ln}^{\text{III}}(\text{Pc})(\text{Pc}^*)]$, Ln = Nd (1), Eu (2), Dy (3), Y (4), and Lu (5). A

Scheme 1. Synthesis of Complexes 1–5: (i) $\text{NH}_3(\text{g})$, NaOMe, MeOH, reflux, 5 h; (ii) PCl_5 , *o*-dichlorobenzene, 110 °C, 1 week; (iii) (a) Et_3N , THF, 0 °C, 12 h; (b) NaOMe, hydroquinone, THF, reflux, 12 h; (iv) $\text{Ln}(\text{OAc})_3 \cdot 4\text{H}_2\text{O}$, DBU, 1-chloronaphthalene



mixture of dried $\text{Ln}(\text{OAc})_3$ (0.08 mmol), 1,8-diazabicyclo[5.4.0]-undec-7-ene (DBU) (1 mL), and 2,3,16,17-tetra(hexylthio)phthalocyanine (H_2Pc , 160 mg, 0.16 mmol) in 1-chloronaphthalene (3 mL) was refluxed under nitrogen for 4 h to give a dark-green solution. After cooling to room temperature, hexane was added dropwise to precipitate the product. The precipitate was filtered through a filter paper and dissolved in CH_2Cl_2 . Purifications by column chromatography on silica gel first and then by preparative thin-layer chromatography eluting with dichloromethane/hexane 1/1 (v/v) afforded the pure products as green solid. Yield: 105 mg for **1** (63%), 106 mg for **2** (63%), 91 mg for **3** (54%), 98 mg for **4** (60%), and 102 mg for **5** (60%). HR-MS (ESI-QTOF) calcd for $\text{C}_{112}\text{H}_{128}\text{NdN}_{16}\text{S}_8$: 2094.7345; found: 2094.7421. Calcd for $\text{C}_{112}\text{H}_{128}\text{EuN}_{16}\text{S}_8$: 2105.7482; found: 2105.7495. Calcd for $\text{C}_{112}\text{H}_{128}\text{DyN}_{16}\text{S}_8$: 2116.7586; found: 2116.7526. Calcd for $\text{C}_{112}\text{H}_{128}\text{YN}_{16}\text{S}_8$: 2041.7327; found: 2041.7235. Calcd for $\text{C}_{112}\text{H}_{122}\text{LuN}_{16}\text{S}_8$: 2127.7676; found: 2127.7665.

Crystallography. Single crystals of **1–5** were obtained by slow diffusion of methanol into concentrated solution in chloroform. Suitable crystals were selected and mounted on a Gemini kappa-geometry diffractometer (Agilent Technologies UK Ltd.) equipped with an Atlas charge-coupled device (CCD) detector and using Mo radiation ($\lambda = 0.71073 \text{ \AA}$). Intensities were collected at 100 K by means of the CrysAlisPro software. Reflection indexing, unit-cell parameters refinement, Lorentz-polarization correction, peak integration, and background determination were carried out with the CrysAlisPro software.²² An analytical absorption correction was applied using the modeled faces of the crystal.²³ The structures were solved by direct methods with SIR97,²⁴ and the least-squares refinement on F^2 was achieved with the CRYSTALS software.²⁵ All non-hydrogen atoms were refined anisotropically. The hydrogen atoms were all located in a difference map, but were then repositioned geometrically. The H atoms were initially refined with soft restraints on the bond lengths and angles to regularize their geometry ($\text{C}\cdots\text{H}$ in the range of 0.93–0.98 Å) and $U_{\text{iso}}(\text{H})$ (in the range of 1.2–1.5 times the U_{eq} value of the parent atom), after which the positions were refined with riding constraints. CCDC 913758 (**1**), 913756 (**2**), 913755 (**3**), and 913759 (**4**) contain the supplementary crystallographic data for this paper.

These data can be obtained free of charge from The Cambridge Crystallographic Data Centre via www.ccdc.cam.ac.uk/data_request/cif. The structure of complex **5** was already reported in a previous paper (CCDC 832167).²¹

Reduction and Oxidation. Reduced species **1b–5b** were obtained in solution by adding NaBH_4 (one crystal) to a solution of complex **1–5** in THF. For the harmonic light scattering (HLS) experiments, solutions of complexes **1–5** in THF were prepared. Then one crystal of NaBH_4 was added. When the color changed from green to blue, the solution was diluted with chloroform to the working concentration and another crystal of NaBH_4 was added. The solutions were filtered through a 0.2 μm membrane filter just before measurement. Oxidized species **1c–5c** were obtained in solution in chloroform by adding a diluted solution of bromine in chloroform.

Hyper-Rayleigh Scattering. A 10^{-5} M solution in CHCl_3 or 10% THF in chloroform were prepared as described above and filtered through a 0.2 μm membrane filter to remove any particles or dust. Fluorescence quartz cells were used for the experiments. Sealable cells purged with argon were used to measure the reduced and oxidized species. The details of the method as well as the experimental set up have been presented previously.^{13d}

RESULTS AND DISCUSSION

Synthesis and X-ray Crystal Structure. 2,3,16,17-Tetra(hexylthio)phthalocyanine was obtained in 8% yield by the selective condensation of 5,6-bis(hexylthio)isoindoline-1,3-diimine with 1,3,3-trichloroisindolenine, followed by oxidation with hydroquinone, as reported.²¹ This method was reported to be regioselective toward the formation of the crosswise ABAB phthalocyanine.²⁶ In our hands however significant amounts of 2,3,9,10,16,17-hexa(hexylthio)phthalocyanine (AB_3) and traces of the symmetric derivative 2,3,9,10,16,17,23,24-octa(hexylthio)phthalocyanines (B_4) were produced that necessitate thorough chromatographic separation from the desired product. The bis(phthalocyanine)lanthanide complexes **1–5**

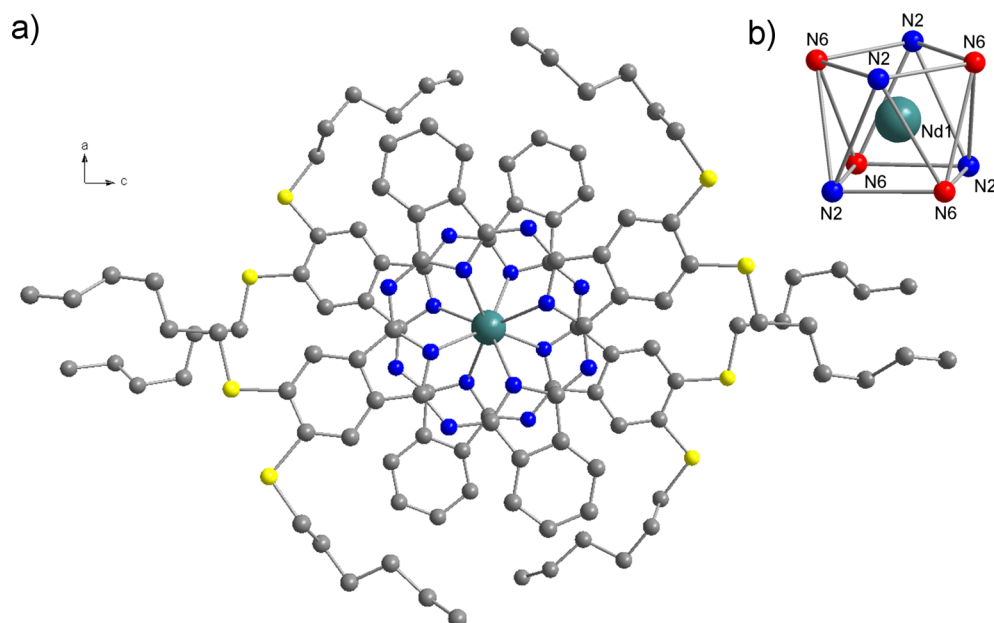


Figure 2. (a) Complex 1 viewed along the b axis (H atoms and disordered C atoms on the hexyl chains are omitted for clarity). (b) Coordination polyhedron around the Nd^{3+} ion. The N_{iso} atoms N(2) and N(6) (N atom of the unsubstituted isoindole ring and of the isoindole ring bearing the electron donating groups, respectively) are pictured in different colors to show the parallel between the coordination polyhedron and the octupolar cube of Figure 1.

Table 1. Selected Crystallographic and Refinement Data for $[\text{Ln}^{\text{III}}(\text{Pc})(\text{Pc}^{\bullet})]$; Ln = Nd (1), Eu (2), Dy (3), Y (4), and Lu (5)

	1	2	3	4	5
formula	$\text{C}_{112}\text{H}_{128}\text{NdN}_{16}\text{S}_8 \cdot 2(\text{CHCl}_3)$	$\text{C}_{112}\text{H}_{128}\text{EuN}_{16}\text{S}_8 \cdot 2(\text{CHCl}_3)$	$\text{C}_{112}\text{H}_{128}\text{DyN}_{16}\text{S}_8 \cdot 2(\text{CHCl}_3)$	$\text{C}_{112}\text{H}_{128}\text{YN}_{16}\text{S}_8 \cdot 2(\text{CHCl}_3)$	$\text{C}_{112}\text{H}_{128}\text{LuN}_{16}\text{S}_8 \cdot 2(\text{CHCl}_3)$
MW (g mol^{-1})	2337.88	2345.60	2356.14	2282.54	2352.48
crystal system	orthorhombic	orthorhombic	orthorhombic	orthorhombic	orthorhombic
space group	$Fddd$	$Fddd$	$Fddd$	$Fddd$	$Fddd$
a (Å)	23.275(1)	23.289(1)	23.1443(2)	23.1860(10)	23.206(5)
b (Å)	29.404(1)	29.342(2)	29.482(3)	29.276(2)	29.202(2)
c (Å)	31.015(2)	31.977(1)	32.219(2)	32.081(2)	31.760(2)
α (deg)	90	90	90	90	90
β (deg)	90	90	90	90	90
γ (deg)	90	90	90	90	90
V (Å ³)	21910(2)	21851(2)	21984(3)	21776(2)	21523(5)
Z	8	8	8	8	8
T (K)	100	100	100	100	100
D_x (g cm^{-3})	1.417	1.426	1.424	1.392	1.452
$R[F^2 > 2\sigma(F^2)]$	0.086	0.067	0.055	0.079	0.059
$wR(F^2)$	0.206	0.127	0.127	0.223	0.170
GOF	0.84	1.07	0.94	0.99	0.96
$p_{\text{min}}/p_{\text{max}}$ (e Å^{-3})	-4.49/4.50	-4.17/2.59	-2.81/1.73	-1.99/1.90	-1.59/2.10
No. reflections	6931	6887	6733	6973	6787
No. parameters	400	401	400	400	400

were obtained in good yield from the ABAB phthalocyanine and lanthanide acetate in refluxing 1-chloronaphthalene, using DBU as a base (see Scheme 1).

X-ray quality crystals of compounds 1–5 can be isolated by letting methanol slowly diffuse in a concentrated chloroform solution, at room temperature for a few days. The X-ray crystallographic analysis revealed that all the complexes are isostructural and identical to the lutetium complex previously described; accordingly, only the crystal structure of 1 (Nd) is shown in Figure 2. Selected crystallographic and refinement data are summarized in Table 1, and important structural parameters are given in Table 2.

Eight double-decker molecules $[\text{Ln}^{\text{III}}(\text{Pc})(\text{Pc}^{\bullet})]$ as well as 16 disordered solvent molecules (CHCl_3) constitute the unit cell. The double-decker $[\text{Ln}^{\text{III}}(\text{Pc})(\text{Pc}^{\bullet})]$ entity consists of two slightly domed phthalocyanine rings flanking a central Ln^{3+} ion. The two macrocycles are staggered with respect to each other, with a staggering angle α of around 45° , which is remarkably constant from Nd to Lu. The entity $[\text{Ln}^{\text{III}}(\text{Pc})(\text{Pc}^{\bullet})]$ is of approximate symmetry D_2 and is therefore chiral. The two enantiomers are present in the crystal structure (Supporting Information, Figure SI-1). The Ln^{3+} ion is octacoordinated by the eight nitrogen atoms of the isoindole N_{iso} (N(2) and N(6)), the polyhedron of the Ln coordination sphere being

Table 2. Selected Structural Data for $[\text{Ln}^{\text{III}}(\text{Pc})(\text{Pc}^{\bullet})]$; Ln = Nd (1), Eu (2), Dy (3), Y (4), and Lu (5)

	1	2	3	4	5
r_8 , pm ^a	110.9	106.6	102.7	101.9	97.7
d_p , Å ^b	2.956	2.841	2.775	2.747	2.656
Ln–N(2), Å ^c	2.477(4)	2.445(4)	2.402(3)	2.400(3)	2.3666(3)
Ln–N(6), Å ^c	2.466(4)	2.428(4)	2.411(3)	2.399(3)	2.356(3)
$\alpha\text{N}(2)$, deg ^{c,d}	45.30	45.30	45.95	45.64	45.37
$\alpha\text{N}(6)$, deg ^{c,e}	44.14	44.10	43.55	44.05	44.43

^aTaken from reference 28. ^bDistance between the upper and lower planes formed by the four isoindole nitrogen atoms N_{iso} (N(2) and N(6)) of each phthalocyanine ring. ^cN(2) and N(6) are the two isoindole nitrogen atoms N_{iso} . N(2) is the N_{iso} of the isoindole moiety bearing the two thioether groups. N(6) is the N_{iso} of the isoindole moiety bearing the hydrogen atoms. ^dAngle between the two planes connecting the metal ion Ln and the two N(2) of each phthalocyanine ring. ^eAngle between the two planes connecting the metal ion Ln and the two N(6) of each phthalocyanine ring.

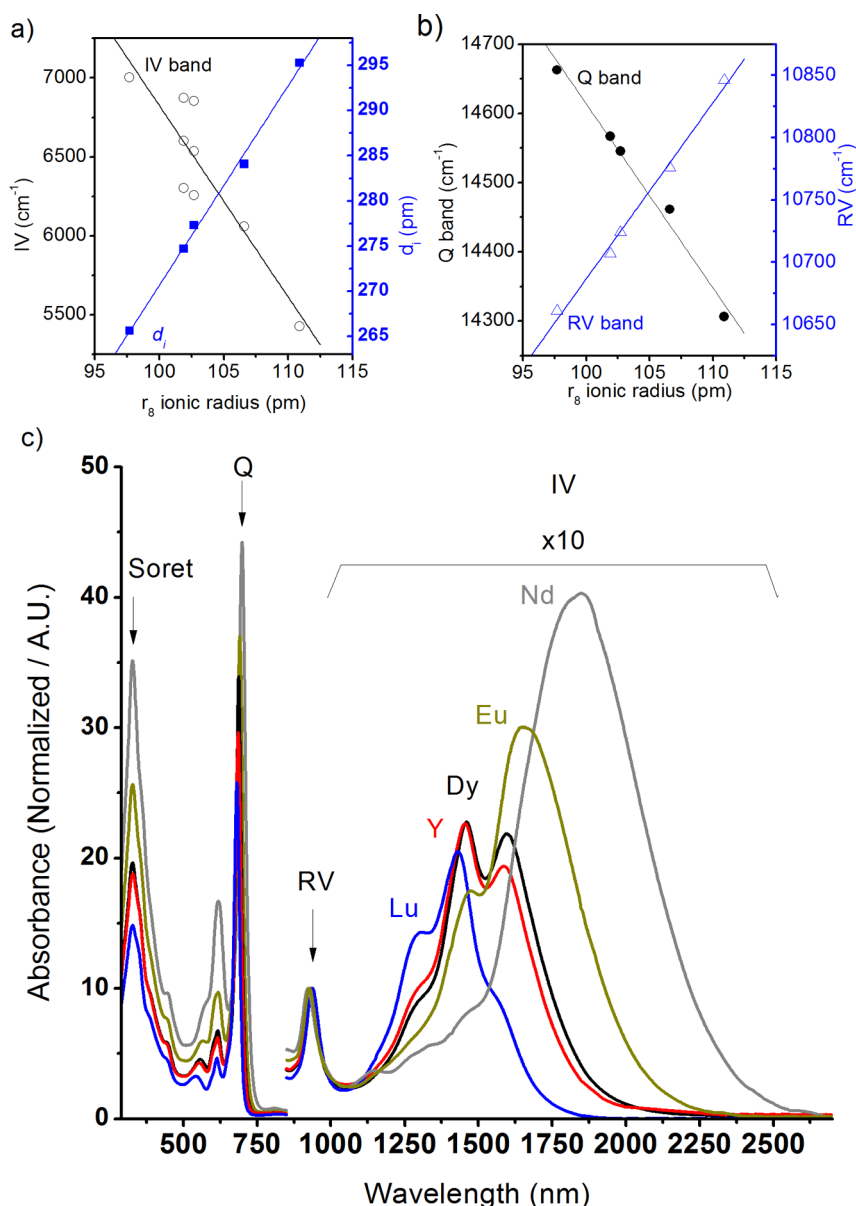


Figure 3. (a) Scatter plot of the ring-to-ring distance (d_i) and of the wavenumber of the intervalence band (IV) against the ionic radius of the eight-coordinated Ln^{3+} ion (r_8). (b) Scatter plot of the red vibronic (RV) band and Q band (Q) against the ionic radius of the eight-coordinated Ln^{3+} ion (r_8). (c) Electronic absorption spectra of the neutral $[\text{Ln}^{\text{III}}(\text{Pc})(\text{Pc}^{\bullet})]$ (Ln = Nd, Eu, Dy, Y, Lu) species 1–5.

best described as a slightly distorted square antiprism. The increase in the size of the metal ion from Lu^{3+} to Nd^{3+} is reflected in the increase of the Ln– N_{iso} distances (from

2.356(3) Å for the shortest distance Lu–N(6) to 2.477(4) Å for the longest distance Nd–N(2)), which is very similar to what was observed for eight-coordinated lanthanide ions in a

Table 3. Electronic Absorption Data (in CHCl₃) and Dynamic Hyperpolarizabilities

complex	Soret band λ_{max} nm	BV band λ_{max} nm	Q band λ_{max} nm	RV band λ_{max} nm	IV band λ_{max} nm	β_{xyz}^a	$\beta_{\text{HLS}}^{b,c}$
1	328	575	699	922	1843	4300	3250
2	329	563	691	928	1650	7180	5430
3	329	556	687	934	1459/1598	7435	5620
4	327	554	686	934	1455/1586	3980	3010
5	327	545	682	938	1431	7620	5760

^aFor an effective octupolar D_2 molecular symmetry: $\beta_{\text{HLS}}^2 = [\langle \beta_{\text{ZZZ}}^2 \rangle + \langle \beta_{\text{YYY}}^2 \rangle] = (4/7)\beta_{\text{xyz}}^2 \cdot \beta_{\text{HLS}}^2$ ($\times 10^{-30}$ esu) determined by hyper-Rayleigh experiments at 1907 nm in CHCl₃ for the mixed-valent complexes [Ln^{III}(Pc)(Pc[•])], where Ln = Nd (1), Eu (2), Dy (3), Y (4), and Lu (5). Reference ethyl violet, $\beta = 170 \times 10^{-30}$ esu at 1907 nm. ^cEstimated error: 15%.

similar structure.²⁷ The interplanar distance d_i , the distance between the two mean planes formed by the four isoindole nitrogen of each macrocycle, increase monotonically with the metal size from 2.656 Å for complex 5 (Lu) to 2.956 Å for complex 1 (Nd). The linear correlation between the d_i distance and the ionic radius of eight-coordinated metal ion (r_8) illustrated in Figure 3²⁸ was already evidenced in diphthalocyaninato(²⁻) metalate complexes of rare earth as well as bismuth, antimony, and indium K[M^{III}(Pc)₂] (M = La, Ce, Pr, Sm, Bi, Sb, In).²⁹ The crystal packing of complexes 1–5 consist of alternating layers of molecules [Ln^{III}(Pc)(Pc[•])] along the packing axis b (as shown in Supporting Information, Figure S.I.-2). As expected the distance between two consecutive layers decreases from 1 (Nd) to 5 (Lu) according to the decrease in the ionic radii. On the other hand, the Ln–Ln distance of two enantiomeric molecules [Ln^{III}(Pc)(Pc[•])] from two consecutive layers, as well as the Ln–Ln distance between two molecules within the same layer, is not directly related to the size of the metal ion, suggesting that other parameters than size govern the crystal packing. The disordered solvent molecules incorporated into the layer of molecules occupying the empty spaces between two disordered alkyl chains (C₆H₁₃) of two adjacent molecules.

Spectroscopic Properties. The electronic absorption spectra of the double-decker complexes 1–5 were recorded in CHCl₃. The data are summarized in Table 3. Figure 3 compares the absorption spectra in the overall 300–2000 nm range. The electronic absorption of lanthanide bis(phthalocyaninates) has been extensively studied and interpreted in terms of mixed-valent compounds. The spectra obtained for compounds 1–5 are typical of such compounds. The Soret bands appear at 328 nm, whereas the intense Q bands are observed in the range of 680–690 nm with vibrational shoulder at 612–618 nm. The Q band is actually the sum of the overlapping Q band of each Pc²⁻ and (Pc[•])⁻ species.^{19b} A small hypsochromic shift is observed for the Q band when the ionic radius of the cation decreases from Nd ($r_8 = 110.9$ pm) to Lu ($r_8 = 97.7$ pm). Compared to simpler unsubstituted [Ln^{III}(Pc)(Pc[•])], the presence of eight electron-donating thioether groups induces a small red shift of all bands. The main characteristic of the electronic absorption spectra of lanthanide bis(phthalocyaninates) is a broad absorption band in the near-infrared region ascribed to an intervalence transition (IV) between the delocalized $b_1 \rightarrow a_2$ HOMO and SOMO.^{17,19a} For complexes 1–5, this intervalence transition appears as a more or less structured band with maxima ranging from 1431 nm for Lu to 1843 nm for Nd. As for the Q band, a linear correlation also exists between the absorption maxima and the ionic radii r_8 (as shown in Figure 3), and therefore the ring-to-

ring separation distance d_i , confirming what was previously reported for simple phthalocyaninato,^{19b} porphyrinato,³⁰ or mixed porphyrinato–naphthalocyaninato³¹ lanthanide double-decker complexes. Transition $1e_g(\pi) \rightarrow a_{1u}(\pi^*)$ from the SOMO-to-LUMO (RV) appears around 925–940 nm and finally transition (BV) from deeper π -bonding $2e_g(\pi)$ level to the SOMO, $2e_g(\pi) \rightarrow a_{1u}(\pi^*)$, gives a band at around 540–560 nm. For these two bands, a small bathochromic shift and a small hypsochromic shift are observed, respectively, when the ring-to-ring distance decreases (Figure 3).

Oxidation and Reduction. The redox properties of double-decker phthalocyanine lanthanide complexes have been extensively studied, and seven³² oxidation states [Ln^{III}Pc₂]^z, with z ranging from –4 to +2, and six one-electron redox-reactions, all involving electrons of the macrocyclic rings, have been characterized in solution.³³ Besides the neutral mixed-valent compound [Ln^{III}(Pc)(Pc[•])], at least two redox states, the one-electron reduced anion [Ln^{III}(Pc)₂]⁻ and the one-electron oxidized cation [Ln^{III}(Pc[•])₂]⁺ are easily accessible chemically. If the structure of the one-electron oxidized cation [Ln^{III}(Pc[•])₂]⁺ has never been reported, quantum chemical study on [Tb^{III}(Pc[•])₂]⁺ based on density functional theory (DFT) revealed a shortened ring-to-ring distance but a conserved staggered conformation on the two phthalocyanine rings.³⁴ Detailed studies were realized on the one-electron reduced anion structure in solution and in the solid state.^{29,35} Koike et al. demonstrated from crystallographic studies of (*n*Bu₄N)[M^{III}(Pc)₂] complexes that, with increasing interplanar distance, the eclipsed conformation of the two cycles would be favored and that the skew angle can even reach 0° if the interplanar distance was longer than the van der Waals distance.^{35a} Analysis of the paramagnetic shifts in proton NMR, correlated with UV–visible spectroscopy, revealed highly symmetrical structures in solution for the nonradical anions of simple phthalocyanine [Ln^{III}(Pc)₂]⁻, probably a staggered form belonging to the D_{4d} point group.^{35c} Homborg et al. showed not only that with large ion size such as Nd³⁺, large d_i distances were sufficient to repulse the steric ligand–ligand interaction but also that the equilibrium between the staggered and the eclipsed conformation was governed by subtle equilibrium forces within the crystal packing.²⁹ In solution then, one can reasonably assume that the octupolar D_2 structure of the neutral species would be conserved at least for the one-electron reduced species. However, in terms of octupolar character, a possible eclipsed conformation would be highly favorable if the substituted isoindole rings are confronted with unsubstituted ones, because this arrangement would then lead to pure T_d symmetry.

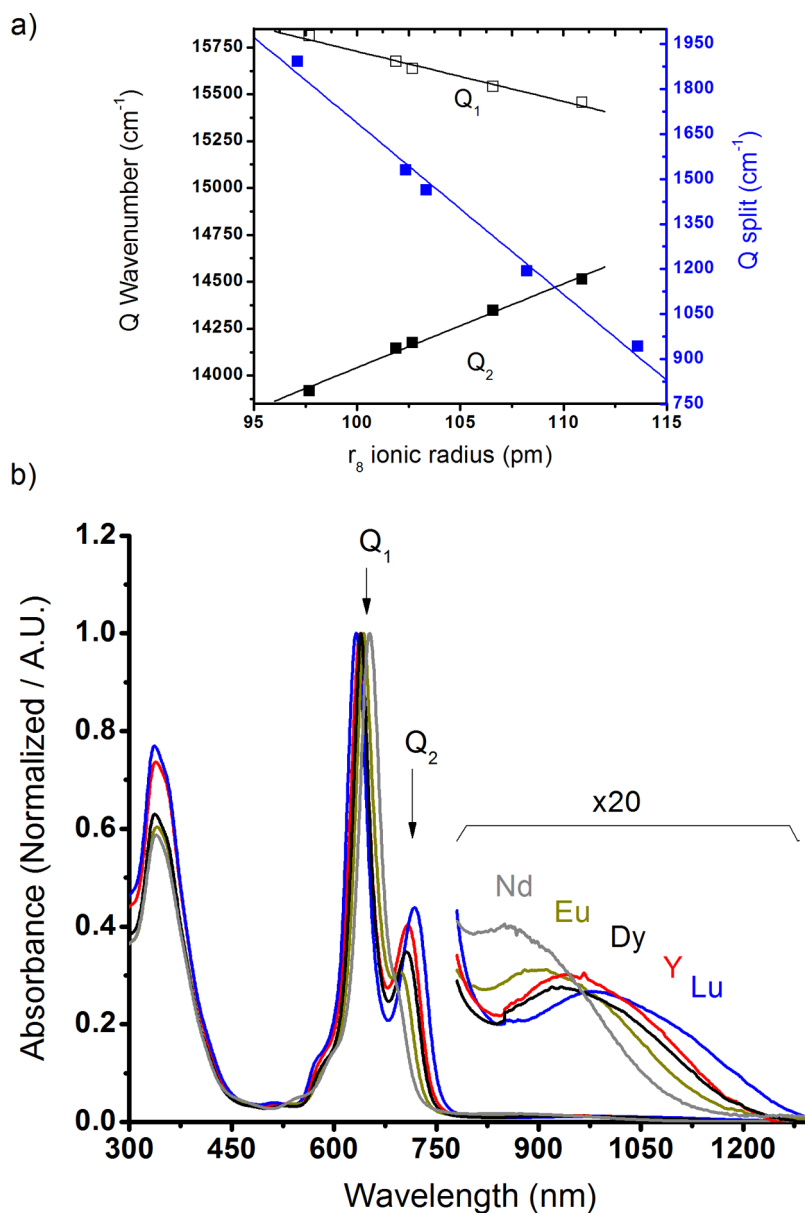


Figure 4. (a) Scatter plot of the wavenumber of the band Q band (Q_1 and Q_2) and of the Q band split against the ionic radius of the eight-coordinated Ln^{3+} ion (r_8). (b) Electronic absorption spectra of the reduced $[\text{Ln}^{\text{III}}(\text{Pc})_2]^-$ ($\text{Ln} = \text{Nd}, \text{Eu}, \text{Dy}, \text{Y}, \text{Lu}$) species **1b–5b** with magnified view of the 850–1300 nm range.

The reduced species $[\text{Ln}^{\text{III}}(\text{Pc})_2]^-$ **1b–5b** ($\text{Ln} = \text{Nd}, \text{Eu}, \text{Dy}, \text{Y}, \text{Lu}$), in which the two phthalocyanine rings are twice negatively charged, were obtained in THF or 10% THF– CHCl_3 solution by reduction of the neutral compounds **1–5** with an excess of NaBH_4 . The solution turned from green to deep blue. The spectral changes associated with chemical reduction are illustrated in Figure 4, and the data are summarized in Table 4. The main spectral feature is the disappearing of all the electronic transitions associated with the phthalocyanine π radical. Therefore the spectra only display three bands: the B band around 335–340 nm, the Q band around 600–700 nm, and a very weak band appearing in the foot of the Q band (Figure 4). The Q band, structured and split into two components, the main band Q_1 and the sideband Q_2 , as already described for simple $[\text{Ln}^{\text{III}}(\text{Pc})_2]^-$ anions,³⁶ also presents a vibronic shoulder at higher energy. As observed for the neutral species, there is a hypsochromic shift of the main Q_1

band and a small bathochromic shift of the side Q_2 band correlated with the ionic radius of the central cation. As a consequence, the splitting of the Q band also correlates well with the interplane distance³⁶ and is much more prominent for the late lanthanide. It has been attributed to increased exciton interaction occurring between the two cycles when the ionic radii decrease. For lighter lanthanide, not only the interaction between the two cycles decreases, but the conformation adopted by the two cycles probably changes.

Upon addition of sodium borodeuteride (NaBD_4) as a reducing agent, well-resolved ¹H NMR spectra were obtained for the reduced form of bis(phthalocyaninato)lanthanide(III) complexes of the diamagnetic cation Y^{3+} (**4b**) and Lu^{3+} (**5b**) in which both macrocyclic ligands become diamagnetic dianions. The two spectra are identical. For these homoleptic compounds, the nonperipheral and peripheral protons of the unsubstituted isoindole ring resonate as four sets of signals as

Table 4. Electronic Absorption Data (in THF) and Dynamic Hyperpolarizabilities

complex	Soret band λ_{\max} nm	Q band		splitting, cm^{-1}	β_{xyz}^c	$\beta_{\text{HLS}}^{a,b}$
		Q_1 λ_{\max} nm	Q_2 λ_{\max} nm			
1b	341	647	689	942	3220	2430
2b	340	643	697	1193	4880	3690
3b	338	639	705	1463	5570	4210
4b	338	638	707	1530	3250	2460
5b	337	632	718	1892	6070	4590

^a β_{HLS} ($\times 10^{-30}$ esu) determined by hyper-Rayleigh experiments at 1907 nm in a mixed solvent system of 10% THF in CHCl_3 for the reduced complexes $[\text{Ln}^{\text{III}}(\text{Pc})_2]^-$, where Ln = Nd (**1b**), Eu (**2b**), Dy (**3b**), Y (**4b**), and Lu (**5b**). Reference ethyl violet, $\beta = 170 \times 10^{-30}$ esu at 1907 nm. ^bEstimated error: 15%. ^cFor an effective octupolar D_2 molecular symmetry: $\beta_{\text{HLS}}^2 = [\langle \beta_{ZZZ}^2 \rangle + \langle \beta_{YZZ}^2 \rangle] = (4/7)\beta_{xyz}^2$.

multiplets, at $\delta = 8.03$ and 8.08 ppm for the peripheral and 8.88 and 8.95 ppm for the nonperipheral protons, respectively, whereas two well-resolved singlets at $\delta = 8.83$ and 8.93 ppm were observed for the nonperipheral protons of the substituted ring. This indicates that a 2-fold symmetry is present in solution, confirmed by the observation of two sets of signals for each CH_2 (and the CH_3) of the thiohexyl chains. For the paramagnetic Eu^{3+} complex (**2b**) the aromatic signals become broader and are shifted to lower field at 9.07 ppm for the peripheral and in the range from 11.09 to 11.27 ppm for all the nonperipheral protons. The SCH_2 protons resonate as two sets of signals at 4.46 and 4.65 ppm. Unfortunately, for the complexes of the paramagnetic cations Nd^{3+} **1b** and Dy^{3+} **3b**, no proper spectra could be obtained.

The oxidized species **1c–5c** (Ln = Nd, Eu, Dy, Y, or Lu) were obtained in CHCl_3 solution by oxidation of the neutral compounds **1–5** with a slight excess of bromine (Br_2), and the solution turned from green to brown. The most probable

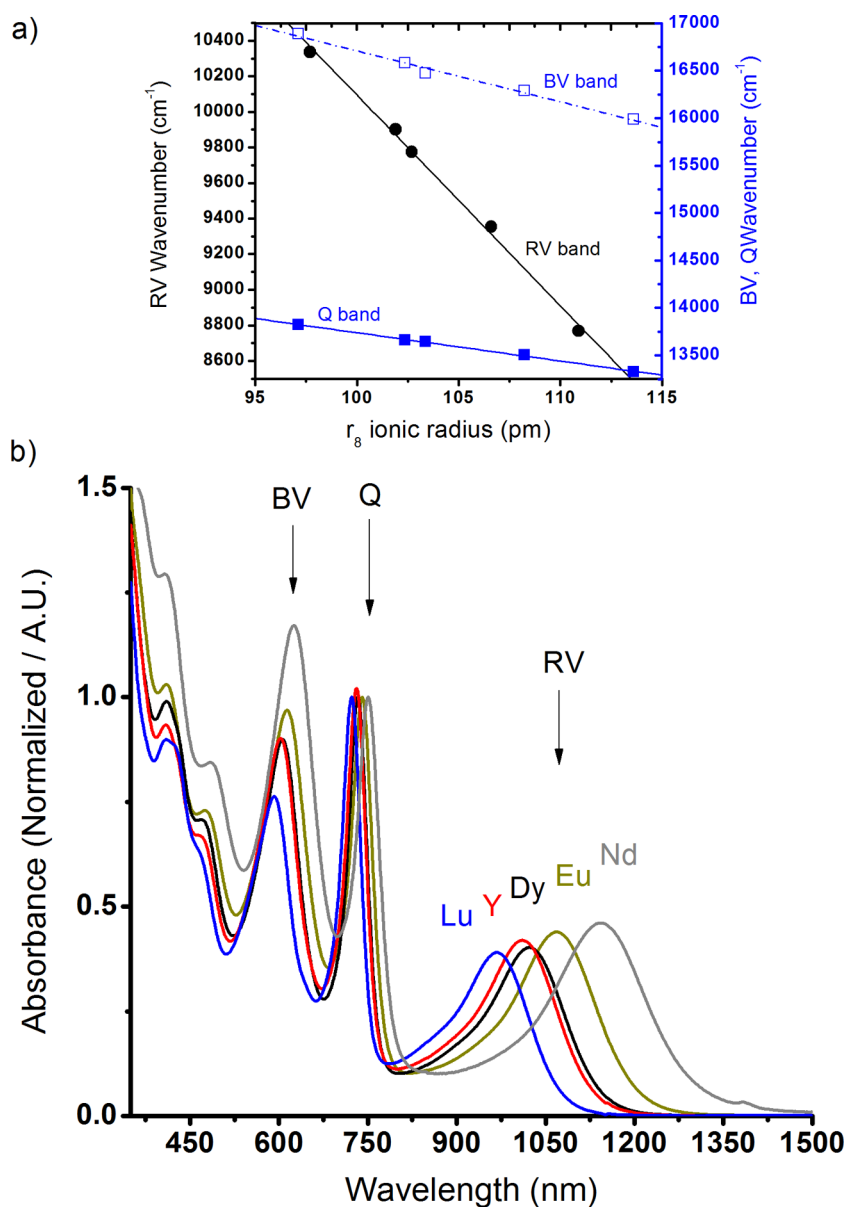


Figure 5. (a) Scatter plot of wavenumber of the red vibronic (RV) band, blue vibronic (BV) band, and Q (Q) band against the ionic radius of the eight-coordinated Ln^{3+} ion (r_8). (b) Electronic absorption spectra of the oxidized $[\text{Ln}^{\text{III}}(\text{Pc}^\bullet)_2]^+$ (Ln = Nd, Eu, Dy, Y, Lu) species **1c–5c**.

structure of the one-electron oxidized species is a complex formed by two π -radical rings (Pc^\bullet).^{27a} The absorption spectra of complexes **1c**–**5c** are shown in Figure 5 and are summarized in Table 5. Besides the B band at 350–400 nm, the strongest Q

Table 5. Electronic Absorption Data (in CHCl_3) and Dynamic Hyperpolarizabilities

	Soret band	BV band	Q band	RV band	β_{xyz}^c	$\beta_{\text{HLS}}^{b,b}$
	λ_{max} nm	λ_{max} nm	λ_{max} nm	λ_{max} nm		
1c	n.d. ^a	625	751	1140	3690	2790
2c	n.d. ^a	614	740	1069	6020	4550
3c	n.d. ^a	607	733	1023	6200	4690
4c	n.d. ^a	603	732	1010	3700	2800
5c	n.d. ^a	592	723	967	6250	4720

^aUnder the residual absorption of Br_2 . ^b β_{HLS} ($\times 10^{-30}$ esu) determined by hyper-Rayleigh experiments at 1907 nm in CHCl_3 for the oxidized complexes $[\text{Ln}^{\text{III}}(\text{Pc}^\bullet)_2]^+$, where Ln = Nd (**1c**), Eu (**2c**), Dy (**3c**), Y (**4c**), and Lu (**5c**). Reference ethyl violet, $\beta = 170 \times 10^{-30}$ esu at 1907 nm. ^bEstimated error 15%. ^cFor an effective octupolar D_2 molecular symmetry: $\beta_{\text{HLS}}^2 = [\langle \beta_{\text{ZZZ}}^2 \rangle + \langle \beta_{\text{YZZ}}^2 \rangle] = (4/7)\beta_{\text{xyz}}^2$

band loses intensity and exhibits a small red shift compared to the neutral form. The transitions characteristic of the π radical at 590–610 nm (BV) and around 1000 nm (RV) increase significantly. Accordingly, the intervalence transition prominent in the neutral form disappeared. Again, for the Q band and the two transitions associated with the π radical, a good linear correlation with the ionic radius was found with hypsochromic shifts observed when the ring-to-ring distance decreases (Figure 5).

■ SECOND-ORDER NONLINEAR OPTICAL PROPERTIES

As previously reported for the lutetium complex **5** the dynamic molecular first hyperpolarizabilities $\sqrt{\langle \beta_{\text{HLS}}^2 \rangle}_{1907}$ of compounds **1**–**4** were determined by nonpolarized HLS (also named hyper-Rayleigh scattering)³⁷ in chloroform solution, using an incident wavelength at 1907 nm. The reference used for the HLS measurements was ethyl violet for which a $\sqrt{\langle \beta_{\text{HLS}}^2 \rangle}_{1907}$ value of 170×10^{-30} esu at 1907 nm was taken.³⁸ If for complexes **3**–**5** (Dy, Y, and Lu) the incident wavelength of 1907 nm was higher than or close to the absorption cutoff of the intervalence band and therefore off-resonance, this is not the case for the other compounds. The europium complex **2** and the neodymium complex **1** especially display quite a strong linear absorption at 1907 nm. Therefore for all compounds, the HLS values were corrected for absorption at 1907 nm by the factor of $10^{A_{1907}}$, A_{1907} being the absorption of the compound at the laser incident wavelength λ_{inc} of 1907 nm. Moreover, note that the scattered light at the second harmonic (953 nm) would be partially absorbed because of the small sharp peak of the RV transition displayed by all compounds around 933 nm. The HLS data were further corrected for by a factor of $10^{A_{953/2}}$, A_{953} being the absorption of the compound solution at the second harmonic wavelength λ_{SHG} of 953 nm. Nevertheless, to minimize the total correction factor applied before determining β_{1907} ($10^{A_{1907}} \times 10^{A_{953/2}} < 3$), very low concentrations (no more than 10^{-5} M) were used. Table 3 lists the dynamic hyperpolarizability $\sqrt{\langle \beta_{\text{HLS}}^2 \rangle}_{1907}$ by HLS obtained at 1907 nm.

First of all, note that the values, ranging from 3010×10^{-30} esu for **4** (Y) to 5760×10^{-30} esu for **5** (Lu), are exceptionally large for hyperpolarizabilities at 1907 nm. The neodymium complex **1** also presents the strongest absorption at 1907 nm but the weakest hyperpolarizability measured for the series at that wavelength. This suggests that the intervalence transition has little influence on the quadratic response as it was already postulated by Shirk et al. for the third-order nonlinear properties of simple $[\text{Ln}^{\text{III}}(\text{Pc})(\text{Pc}^\bullet)]$.³⁹

The structures of complexes **1**–**5** in solution were not determined; however, ¹H NMR studies on homoleptic and heteroleptic diphthalocyaninato(²⁻) metalate complexes $[\text{Ln}^{\text{III}}(\text{Pc})_2]^-$ of rare earth have shown that the solid-state structure was preserved in solution at least for the smaller ions^{35c} even if the two rings are free to rotate with respect to each other. Thus, we can reasonably assume an effective octupolar D_2 molecular symmetry in solution for complexes **1**–**5**. In that symmetry group, there are six nonzero tensor components β_{xyz} contributing to the total HLS signal related to the observable by the following relationships:

$$\beta_{\text{HLS}}^2 = [\langle \beta_{\text{ZZZ}}^2 \rangle + \langle \beta_{\text{YZZ}}^2 \rangle] = \frac{4}{7}\beta_{\text{xyz}}^2 \quad (1)$$

Calculation gave values ranging from 3980×10^{-30} esu for **4** (Y) to 5760×10^{-30} esu for **5** (Lu), much higher than those obtained for any octupolar chromophores. Actually, to the best of our knowledge, these are the largest values ever reported for nondipolar compounds, higher than the best octupolar molecules described to date.¹⁵

The second important observation is the increase of the hyperpolarizability values with the number of f electron. The enhancement of the second-order nonlinear response as a function of the number of f electrons was initially reported on dipolar complexes of dibutylaminophenyl-functionalized annulated terpyridine ligand^{14a,c} and on D_{3d} octupolar complexes of dipicolinic acid.^{14b} Theoretical calculation involved the polarization of the 4f electrons in these Ln complexes of push–pull ligand of a rather polarizable ligand to explain the enhancement observed.^{14c,40} More recently, study on lanthanide complexes of hexafluoroacetylacetonate and diglyme, $[\text{Ln}(\text{hfac})_3(\text{diglyme})]$, two ligands lacking a charge-transfer transition, confirmed the tuning of the second-order nonlinear properties by the f electrons and emphasized the unexpected polarizable character of f electrons.⁴¹ It also showed that the influence of the f electrons on the molecular quadratic hyperpolarizability was much higher for the dipolar contribution than for the octupolar contribution, although the major contribution to the total quadratic hyperpolarizability was the octupolar one. In our case, the influence of the number of f electrons on the hyperpolarizability is perfectly illustrated by the difference observed between the dysprosium and the yttrium complexes **3** and **4**. The Y^{3+} and Dy^{3+} ions have similar ionic radii ($r_8 = 1.019$ and 1.027 Å, respectively),²⁸ and the two complexes have similar optical properties. However, Yttrium is not a 4f-block element and therefore Y^{3+} has a $4f^0$ electronic configuration compared to the $4f^9$ electronic configuration of Dy^{3+} . As a consequence, the quadratic hyperpolarizability of **4** is 1.9 times lower than that of **3** in relation to the f-electron polarizable character. However, it is worth noting that the neodymium complex **1** has a similar value to **4** when it should be higher (Nd^{3+} has a $4f^4$ configuration). This seems to indicate that the second-order nonlinear responses of complexes **1**–**5** are not only driven by

the f-electron polarization but also indirectly by geometrical parameters such as the metal ionic radius.

The dynamic molecular first hyperpolarizabilities $\sqrt{\langle\beta_{\text{HLS}}^2\rangle}_{1907}$ of all the reduced $[\text{Ln}^{\text{III}}(\text{Pc})_2]^-$ and oxidized $[\text{Ln}^{\text{III}}(\text{Pc}^\bullet)_2]^+$ species **1b–5b** and **1c–5c** have also been measured by nonpolarized HLS and are given in Tables 4 and 5. The absorptions of the compounds at the laser incident wavelength ($\lambda = 1907$ nm) and at the second-harmonic signal ($\lambda = 953$ nm) were less problematic than they were for the neutral compounds. Nevertheless, the measurements were done in dilute solution (10% THF in CHCl_3 or CHCl_3), at the same concentration (10^{-5} M), to obtain values that can be directly compared with the previous ones regardless of concentration effects. For a given metal ion, very similar values were obtained for the reduced and oxidized form (except for Eu). For all metal ions, however, the values obtained are somewhat lower than those of the neutral form. Nevertheless, they remain exceptionally large for octupolar molecules. Analyzing the total HLS value β_{HLS}^2 in an effective D_2 molecular symmetry using eq 1 gave values of β_{xyz} in the range from 3220 to 6070×10^{-30} esu for **1b–5b** and 3690 to 6250×10^{-30} esu for **1c–5c** of the same order of magnitude as for the supermolecular chromophores described by Therien and Clays.¹⁵ The hyperpolarizabilities of the reduced species **1b–5b** regularly increased from Nd to Lu following the 4f orbital filling. The enhancement factor calculated between **3b** (Dy, $4f^9$) and **4b** (Y, $4f^0$) was somewhat lower than the 1.9 obtained for the neutral form, but comparable with the 1.5 reported in the literature.^{14a,b} However, the value for **4b** is the same as the one for **1b** (Nd, $4f^8$), suggesting that, as already noticed for the neutral form, the interaction between the two macrocycles (related to the interplane distance hence the metal size) is another important parameter controlling the hyperpolarizability. The same observations can be made for the hyperpolarizability values measured for the oxidized species **1c–5c**. The enhancement factor between **3c** (Dy, $4f^9$) and **4c** (Y, $4f^0$) is 1.6. The increase of the hyperpolarizability values resembles the one observed for the neutral form, with a big difference between neodymium and europium and then a regular increase to lutetium. In that case, note that the incident wavelength at 1907 nm comes into resonance with one of the π -radical transitions centered at around 1000 nm. This band is not an intervalence transition, and hence two-photon enhancement in the hyperpolarizability cannot be ruled out. Given the blue shift observed for this transition when the ionic radius decreases, this effect would be more pronounced for the lighter lanthanides.

CONCLUSION

A series of octupolar nonlinear optical chromophores have been synthesized based on double-decker lanthanide (III) complexes of crosswise ABAB phthalocyanine ligands bearing thioether electron donor group and hydrogen atoms alternatively on the macrocycle. This 3D structure was designed to closely match the structure of the octupolar cube, the delocalization between the two rings approximating to the electronic interaction along the edges of the cube. The D_2 noncentrosymmetric structure was confirmed by X-ray diffraction studies. The size of the lanthanide (III) central ion modulates the ring-to-ring distance and the degree of coupling between the two phthalocyanine rings and consequently modulates the optical properties of the chromophore, in particular the strong near-infrared absorption due to the

intervalence transition between the two rings. These potent nonlinear chromophores exhibit exceptionally large dynamic molecular first hyperpolarizabilities $\sqrt{\langle\beta_{\text{HLS}}^2\rangle}_{1907}$ as determined by nonpolarized HLS in solution at 1907 nm, among the highest ever measured. That laser wavelength comes in resonance with the intervalence band in the case of the larger ion complexes (Nd^{3+} and Eu^{3+}). Despite that, the lutetium complex presents the highest hyperpolarizability over the lanthanide series, which seems to indicate that the intervalence transition has little influence on the quadratic nonlinear response. On the other hand, the dynamic molecular first hyperpolarizabilities values show the dependence with the number of the 4f electrons already observed on lanthanide (III) octupolar complexes of other symmetries attributed to the polarizable character of f electrons.⁴⁰ Finally, the one-electron oxidized and the one-electron reduced complexes were studied. Owing to the different oxidation states on the macrocycles, the oxidized and reduced species display considerably changed optical properties compared to the neutral states while keeping a similar octupolar structure. The dynamic molecular first hyperpolarizabilities measured at 1907 nm remain exceptionally large for such simple structures, emphasizing the interest of this original octupolar design. This work represents a first step toward the elaboration of fully cubic octupolar architectures. In that prospect, work on crosswise phthalocyanine bearing true electron withdrawing groups has started. The one-electron reduced species are particularly appealing because, as suggested by the works by Koike^{35a} and Homborg,²⁹ diphthalocyaninato-(²⁻)metallate(III) complexes display conformational heterogeneity depending on the size of the central metal ion and of the counteranion. In particular, in the case of ions larger in size than Nd^{3+} , such as La^{3+} or Bi^{3+} , eclipsed conformation of the two cycles can be obtained on the occasion of slightly different interactions of the anions and the cations. Work in that direction has also started.

ASSOCIATED CONTENT

Supporting Information

Additional figures, HR-MS data and spectra, NMR spectra, and X-ray crystallographic data. This material is available free of charge via the Internet at <http://pubs.acs.org>.

AUTHOR INFORMATION

Corresponding Authors

*E-mail: chirel@gyte.edu.tr (C.H.).

*E-mail: yann.bretonniere@ens-lyon.fr (Y.B.).

Funding

This work was supported by TÜBİTAK 1001 Project 108M034 and the French Embassy in Turkey (Ph.D. fellowship to M.M.A.).

Notes

The authors declare no competing financial interest.

REFERENCES

- (1) (a) Dalton, L. R. *J. Phys.: Condens. Matter* **2003**, *15*, R897–R934. (b) Bentoumi, W.; Mulatier, J.-C.; Bouit, P.-A.; Maury, O.; Barsella, A.; Vola, J.-P.; Chastaing, E.; Divay, L.; Soyer, F.; Le Barny, P.; Bretonnière, Y.; Andraud, C. *Submitted for publication*.
- (2) Zyss, J. *J. Chem. Phys.* **1992**, *98*, 6583–6599.
- (3) (a) Zyss, J. *Nonlinear Opt.* **1991**, *1*, 3–18. (b) Zyss, J.; Ledoux, I. *Chem. Rev.* **1994**, *94*, 77–105.
- (4) Kim, H. M.; Cho, B. R. *J. Mater. Chem.* **2009**, *19*, 7402–7409.

- (5) (a) Chandra Ray, P.; Kumar Das, P. *Chem. Phys. Lett.* **1995**, *244*, 153–156. (b) Stadler, S.; Bräuchle, C.; Brandl, S.; Gompper, R. *Chem. Mater.* **1996**, *8*, 676–678. (c) Brasselet, S.; Cherioux, F.; Audebert, P.; Zyss, J. *Chem. Mater.* **1999**, *11*, 1915–1920. (d) Cho, B. R.; Park, S. B.; Lee, S. J.; Son, K. H.; Lee, S. H.; Lee, M.-J.; Yoo, J.; Lee, Y. K.; Lee, G. J.; Kang, T. I.; Cho, M.; Jeon, S.-J. *J. Am. Chem. Soc.* **2001**, *123*, 6421–6422. (e) Alcaraz, G.; Euzenat, L.; Mongin, O.; Katan, C.; Ledoux, I.; Zyss, J.; Blanchard-Desce, M.; Vaultier, M. *Chem. Commun.* **2003**, 2766–2767. (f) Brunel, J.; Mongin, O.; Jutand, A.; Ledoux, I.; Zyss, J.; Blanchard-Desce, M. *Chem. Mater.* **2003**, *15*, 4139–4148. (g) Cui, Y. Z.; Fang, Q.; Lei, Xue, G.; Yu, W. T. *Chem. Phys. Lett.* **2003**, *377*, 507–511. (h) Traber, B.; Wolff, J. J.; Rominger, F.; Oeser, T.; Gleiter, R.; Goebel, M.; Wortmann, R. *Chem.—Eur. J.* **2004**, *10*, 1227–1238. (i) Hennrich, G.; Asselberghs, I.; Clays, K.; Persoons, A. *J. Org. Chem.* **2004**, *69*, 5077–5081. (j) Quintiliani, M.; García-Frutos, E. M.; Gouloumis, A.; Vázquez, P.; Ledoux-Rak, I.; Zyss, J.; Claessens, C. G.; Torres, T. *Eur. J. Org. Chem.* **2005**, *2005*, 3911–3915. (k) Piao, M. J.; Chajara, K.; Yoon, S. J.; Kim, H. M.; Jeon, S.-J.; Kim, T.-H.; Song, K.; Asselberghs, I.; Persoons, A.; Clays, K.; Cho, B. R. *J. Mater. Chem.* **2006**, *23*, 2273–2281. (l) Argouarch, G.; Veillard, R.; Roisnel, T.; Amar, A.; Boucekkine, A.; Singh, A.; Ledoux, I.; Paul, F. *New J. Chem.* **2011**, *35*, 2409–2411. (m) Moreno Oliva, M.; Juárez, R.; Ramos, M.; Segura, J. L.; van Cleuvenbergen, S.; Clays, K.; Goodson, I.; Theodore; López Navarrete, J. T.; Casado, J. *J. Phys. Chem. C* **2013**, *117*, 626–632.
- (6) Ratera, I.; Ruiz-Molina, D.; Sporer, C.; Marcen, S.; Montant, S.; Létard, J.-F.; Freysz, E.; Rovira, C.; Veciana, J. *Polyhedron* **2012**, *22*, 1851–1856.
- (7) (a) Stadler, S.; Feiner, F.; Bräuchle, C.; Brandl, S.; Gompper, R. *Chem. Phys. Lett.* **1995**, *245*, 292–296. (b) Stadler, S.; Bräuchle, C.; Brandl, S.; Gompper, R. *Chem. Mater.* **1996**, *8*, 414–417.
- (8) (a) Lambert, C.; Schmäzlin, E.; Meerholz, K.; Bräuchle, C. *Chem.—Eur. J.* **1998**, *4*, 512–521. (b) Bourgogne, C.; Le Fur, Y.; Juen, P.; Masson, P.; Nicoud, J.-F.; Masse, R. *Chem. Mater.* **2000**, *12*, 1025–1033. (c) Quintiliani, M.; Pérez-Moreno, J.; Asselberghs, I.; Vázquez, P.; Clays, K.; Torres, T. *J. Phys. Chem. C* **2010**, *114*, 6309–6315.
- (9) Blanchard-Desce, M.; Baudin, J.-B.; Ruel, O.; Jullien, L.; Brasselet, S.; Zyss, J. *Opt. Mater.* **1998**, *9*, 276–279.
- (10) (a) Sastre, A.; Torres, T.; Diaz-García, M. A.; Agulló-López, F.; Dhenaut, C.; Brasselet, S.; Ledoux, I.; Zyss, J. *J. Am. Chem. Soc.* **1996**, *118*, 2746–2747. (b) Kang, S. H.; Kang, Y.-S.; Zin, W.-C.; Olbrechts, G.; Wostyn, K.; Clays, K.; Persoons, A.; Kim, K. *Chem. Commun.* **1999**, 1661–1662. (c) Olbrechts, G.; Wostyn, K.; Clays, K.; Persoons, A.; Kang, S. H.; Kim, K. *Chem. Phys. Lett.* **1999**, *308*, 173–175. (d) Martín, G.; Rojo, G.; Agulló-López, F.; Ferro, V. R.; García de la Vega, J. M.; Martínez-Díaz, M. V.; Torres, T.; Ledoux, I.; Zyss, J. *J. Phys. Chem. B* **2002**, *106*, 13139–13145. (e) Claessens, C. G.; González-Rodríguez, D.; Torres, T.; Martín, G.; Agulló-López, F.; Ledoux, I.; Zyss, J.; Ferro, V. R.; García de la Vega, J. M. *J. Phys. Chem. B* **2005**, *109*, 3800–3806.
- (11) Zyss, J.; Dhenaut, C.; Chauvan, T.; Ledoux, I. *Chem. Phys. Lett.* **1993**, *206*, 409–414.
- (12) Lequan, M.; Branger, C.; Simon, J.; Thami, T.; Chauchard, E.; Persoons, A. *Adv. Mater.* **1994**, *6*, 851–853.
- (13) (a) Dhenaut, C.; Ledoux, I.; Samuel, I. D. W.; Zyss, J.; Bourgalet, M.; Le Bozec, H. *Nature* **1995**, *374*, 339–342. (b) Evans, C. C.; Masse, R.; Nicoud, J.-F.; Bagieu-Beucher, M. *J. Mater. Chem.* **2000**, *10*, 1419–1423. (c) Feuvrie, C.; Maury, O.; Le Bozec, H.; Ledoux, I.; Morrall, J. P.; Dalton, G. T.; Samoc, M.; Humphrey, M. G. *J. Phys. Chem. A* **2001**, *111*, 8980–8985. (d) Maury, O.; Viau, L.; Sénéchal, K.; Corre, B.; Guégan, J.-P.; Renouard, T.; Ledoux, I.; Zyss, J.; Le Bozec, H. *Chem.—Eur. J.* **2004**, *4454*–4466.
- (14) (a) Sénéchal, K.; Toupet, L.; Ledoux, I.; Zyss, J.; Le Bozec, H.; Maury, O. *Chem. Commun.* **2005**, 2180–2181. (b) Tancrez, N.; Feuvrie, C.; Ledoux, I.; Zyss, J.; Toupet, L.; Le Bozec, H.; Maury, O. *J. Am. Chem. Soc.* **2005**, *127*, 13474–13475. (c) Sénéchal-David, K.; Hemeryck, A.; Tancrez, N.; Toupet, L.; Williams, J. A. G.; Ledoux, I.; Zyss, J.; Boucekkine, A.; Guégan, J.-P.; Le Bozec, H.; Maury, O. *J. Am. Chem. Soc.* **2006**, *128*, 12243–12255.
- (15) Ishizuka, T.; Sinks, L. E.; Song, K.; Hung, S.-T.; Nayak, A.; Clays, K.; Therien, M. J. *J. Am. Chem. Soc.* **2011**, *133*, 2884–2896.
- (16) Bartholomew, G. P.; Ledoux, I.; Mukamel, S.; Bazan, G. C.; Zyss, J. *J. Am. Chem. Soc.* **2002**, *124*, 13480–13485.
- (17) Weiss, R.; Fischer, J. Lanthanide Phthalocyanine Complexes. In *The Porphyrin Handbook*; Kadish, K. M.; Smith, K. M.; Guillard, R., Eds.; Academic Press, Elsevier: Amsterdam, Boston, London, New York, Oxford, Paris, San Diego, San Francisco, Singapore, Sydney, Tokyo, 2003; Vol. 16, pp 171–246.
- (18) (a) Corker, G. A.; Grant, B.; Clecak, N. J. *J. Electrochem. Soc.* **1979**, *126*, 1339–1343. (b) Orti, E.; Brédas, J. L.; Clarisse, C. *J. Phys. Chem.* **1990**, *92*, 1228–1235.
- (19) (a) VanCott, T. C.; Gasyina, Z.; Schatz, P. N.; Boyle, M. E. *J. Phys. Chem.* **1995**, *99*, 4820–4830. (b) Ostendorp, G.; Homborg, H. *Z. Anorg. Allg. Chem.* **1996**, *622*, 1222–1230.
- (20) (a) La Mar, G. N.; de Ropp, J. S.; Smith, K. M.; Langry, K. C. *J. Am. Chem. Soc.* **1980**, *102*, 4835–4836. (b) De Cian, A.; Moussavi, M.; Fisher, J.; Weiss, R. *Inorg. Chem.* **1985**, *24*, 3162–3167.
- (21) Ayhan, M. M.; Singh, A.; Hirel, C.; Gürek, A. G.; Ahsen, V.; Jeanneau, E.; Ledoux-Rak, I.; Zyss, J.; Andraud, C.; Bretonnière, Y. *J. Am. Chem. Soc.* **2012**, *134*, 3655–3658.
- (22) *CrysAlisPro*, Version 1.171.35.21 (release 20–01–2012 *CrysAlis171.NET*); Agilent Technologies: Santa Clara, CA, compiled Jan 23, 2012, 18:06:46.
- (23) Clark, R. C.; Reid, J. S. *Acta Crystallogr.* **1995**, *A51*, 887–897.
- (24) Altomare, A.; Burla, M. C.; Camalli, M.; Cascarano, G. L.; Giacovazzo, C.; Guagliardi, A.; Moliterni, A. G. G.; Polidori, G.; Spagna, R. *J. Appl. Crystallogr.* **1999**, *32*, 115–119.
- (25) Betteridge, P. W.; Carruthers, J. R.; Cooper, R. I.; Prout, K.; Watkin, D. J. *J. Appl. Crystallogr.* **2003**, *36*, 1487.
- (26) (a) Idelson, E. M. Novel tetrazaporphins. U.S. Patent US004061654, 1977.12.6, 1977. (b) Young, J. G.; Onyebuagu, W. J. *Org. Chem.* **1990**, *55*, 2155–2159.
- (27) (a) Gürek, A. G.; Ahsen, V.; Luneau, D.; Pécaut, J. *Inorg. Chem.* **2001**, *40*, 4793–4797. (b) Jiang, J.; Bian, Y.; Furuya, F.; Liu, W.; Choi, M. T. M.; Kobayashi, N.; Li, H.-W.; Yang, Q.; Mak, T. C. W.; Ng, D. K. P. *Chem.—Eur. J.* **2001**, *7*, 5059–5069. (c) Lu, G.; Bai, M.; Li, R.; Zhang, X.; Ma, C.; Lo, P.-C.; Ng, D. K. P.; Jiang, J. *Eur. J. Inorg. Chem.* **2001**, *3703*–3709. (d) Gürek, A. G.; Basova, T.; Luneau, D.; Lebrun, C.; Kol'tsov, E.; Hassan, A. K.; Ahsen, V. *Inorg. Chem.* **2006**, *45*, 1667–1676. (e) Zhou, Y.; Zhang, Y.; Wang, H.; Jiang, J.; Bian, Y.; Muranaka, A.; Kobayashi, N. *Inorg. Chem.* **2009**, *48*, 8925–8933. (f) Katoh, K.; Komeda, T.; Yamashita, M. *Dalton Trans.* **2010**, *39*, 4708–4723.
- (28) Shannon, R. D. *Acta Crystallogr.* **1976**, *32*, 751–767.
- (29) Hückstädt, H.; Tutaß, A.; Goldmer, M.; Cornelissen, U.; Homborg, H. *Z. Anorg. Allg. Chem.* **2001**, *627*, 485–497.
- (30) Buchler, J. W.; Scharbert, B. *J. Am. Chem. Soc.* **1988**, *110*, 4272–4276.
- (31) Bian, Y.; Wang, D.; Wang, R.; Weng, L.; Dou, J.; Zhao, D.; Ng, D. K. P.; Jiang, J. *New J. Chem.* **2003**, *27*, 844–847.
- (32) (a) Yilmaz, I.; Nakanishi, T.; Gürek, A. G.; Kadish, K. M. *J. Porphyrins Phthalocyanines* **2003**, *7*, 227–238. (b) Zhu, P.; Lu, F.; Pan, N.; Arnold, D. P.; Zhang, S.; Jiang, J. *Eur. J. Inorg. Chem.* **2004**, *2004*, 510–517.
- (33) L'Her, M.; Pondaven, A. Electrochemistry of Phthalocyanines. In *The Porphyrin Handbook*; Kadish, K. M.; Smith, K. M.; Guillard, R., Eds. Academic Press: New York, 2003; Vol. 16, pp 117–170.
- (34) Takamatsu, S.; Ishikawa, N. *Polyhedron* **2007**, *26*, 1859–1862.
- (35) (a) Koike, N.; Uekusa, H.; Ohashi, Y.; Harnood, C.; Kitamura, F.; Ohsaka, T.; Tokuda, K. *Inorg. Chem.* **1996**, *35*, 5798–5804. (b) Gonidec, M.; Amabilino, D. B.; Veciana, J. *Dalton Trans.* **2012**, *41*, 13632–13639. (c) Konami, H.; Hatano, M.; Tajiri, A. *Chem. Phys. Lett.* **1989**, *160*, 163–167.
- (36) Liu, W.; Jiang, J.; Du, D.; Arnold, D. P. *Aust. J. Chem.* **2000**, *53*, 131–135.
- (37) (a) Clays, K.; André, P. *Phys. Rev. Lett.* **1991**, *66*, 2980–2983. (b) Clays, K.; Persoons, A. *Rev. Sci. Instrum.* **1992**, *63*, 3285–3289.
- (38) Le Bozec, H.; Le Boudier, T.; Maury, O.; Bondon, A.; Ledoux, I.; Deveau, S.; Zyss, J. *Adv. Mater.* **2001**, *13*, 1677–1681.

(39) (a) Shirk, J. S.; Lindle, J. R.; Bartoli, F. J.; Boyle, M. E. *J. Phys. Chem.* **1992**, *96*, 5847–5852. (b) Shirk, J. S.; Lindle, J. R.; Bartoli, F. J.; Hoffman, C. A.; Kafafi, Z. H.; Snow, A. W. *Appl. Phys. Lett.* **1989**, *55*, 1287–1288.

(40) Furet, E.; Costuas, K.; Rabiller, P.; Maury, O. *J. Am. Chem. Soc.* **2008**, *130*, 2180–2183.

(41) Valore, A.; Cariati, E.; Righetto, S.; Roberto, D.; Tessore, F.; Ugo, R.; Fragalà, I. L.; Fragalà, M. E.; Malandrino, G.; De Angelis, F.; Belpassi, L.; Ledoux-Rak, L.; Hoang-Thi, K.; Zyss, J. *J. Am. Chem. Soc.* **2010**, *132*, 4966–4970.